

Variations of the He II $\lambda 1640$ line in B0e–B2.5e stars

M. A. Smith

Science Programs, Computer Sciences Corporation, Space Telescope Science Institute, 3700 San Martin Dr., Baltimore, MD 21218, USA
e-mail: msmith@stsci.edu

Received 20 February 2006 / Accepted 1 August 2006

ABSTRACT

Using the *International Ultraviolet Explorer* data archive, we have examined the SWP echellograms of 74 B0–B2.5e stars for statistically significant fluctuations in the He II (“H α ”) $\lambda 1640$ line profile. In this sample we found that the He II line is occasionally variable in 10 stars over short to long timescales. The He II-variable stars discovered are λ Eri, ω Ori, μ Cen, 6 Cep, HD 67536, ψ^1 Ori, η Cen, π Aqr, 2 Vul, and 19 Mon. The most frequent two types of variability are an extended blue wing absorption and a weakening of the line along the profile. Other types of variability are a weak emission in the red wing and occasionally a narrow emission feature. In the overwhelming number of cases, the CIV resonance doublet exhibits a similar response; rarely, it can exhibit a variation in the opposite sense. Similar responses are also often seen in the Si IV doublet, and occasionally even the Si III $\lambda 1206$ line. We interpret the weakenings of He II and of high-velocity absorptions of CIV to localized decreases in the photospheric temperature, although this may not be a unique interpretation. We discuss the variable blue wing absorptions and red wing emissions in terms of changes in the velocity law and mass flux carried by the wind. In the latter case, recent experimental models by Venero, Cidale, & Ringuélet require that during such events the wind must be heated by 35 000 K at some distance from the star.

Key words. stars: general – stars: emission-line, Be – stars: winds, outflows – ultraviolet: stars

1. Introduction

Together with the hydrogen lines, the lines of helium are among the most important in the spectra of hot stars. In atmospheres of B stars and most O stars, the dominant ion stage of helium is He⁺, and the strongest of the He II features is the $\lambda 1640$ (“H α ”) line. In O stars this line is formed substantially in the wind – so much so in supergiants that the line generally develops a strong P Cygni emission structure. For spectral types later than O8–O9, the line decreases in strength, but it remains visible as a photospheric diagnostic for spectra as late as B2.5 (Peters 1990; Rountree & Sonneborn 1991).

The He II $\lambda 1640$ line is actually a complex of seven permitted transitions arising from lower levels at 40.8 eV. Its effective centroid wavelength is 1040.42 Å. In the outer atmospheres of hot stars this line is formed by the photoionization of He²⁺ by extreme UV (< $\lambda 228$) photons, followed by recombination. The density and temperature sensitivities insures that the line’s formation occurs substantially in the base of the wind or within the photosphere for O and B stars near the main sequence, respectively.

The $\lambda 1640$ line is mildly sensitive to departures from LTE in the He¹⁺ atom. As a result, the strengths computed from non-LTE models tend to be slightly stronger than those from LTE models. Since these effects are relatively small, there appears to be no major difficulties fitting this line approximately with conventional blanketed non-LTE model atmospheres. Auer & Mihalas (1972) suggested that the near coincidence of central wavelengths of the He II and some hydrogen lines could enhance emission of He II $\lambda 4686$ and $\lambda 1640$ through optical pumping (Bowen fluorescence). However, using more recent atomic parameters, Herrero (1987) demonstrated that these effects are negligible. Recently, Venero et al. (2000; “VCR”) have considered

the behavior of the $\lambda 1640$ line for model atmospheres with $T_{\text{eff}} = 25\,000$ K and strong, isotropic, and heated winds. These authors find that even for model atmospheres of early-type B stars a fast and/or heated wind can alter the underlying photospheric profile. For example, in these models $\lambda 1640$ undergoes a near maximum *absorption* strength in winds having a temperature determined by radiative equilibrium, i.e., with $T_0/T_{\text{eff}} = 0.6$ – 0.8 . However, if the wind is heated to 10 000 K above the T_{eff} , then emissions will be produced in one or both of the line wings. Thus, isotropic, heated ($T_0 \geq T_{\text{eff}}$) winds produce a P Cygni-type profile, that is, with a distinctly blueshifted absorption and slightly redshifted emission. For standard wind models for early-type Be stars (unheated winds, with $\dot{M} \sim 1 \times 10^{-8} M_{\odot} \text{ yr}^{-1}$), emission should be absent or undetectable. Even in the spectrum of the O9 V star 10 Lac, with its mass loss rate of $1.7 \times 10^{-7} M_{\odot} \text{ yr}^{-1}$, the $\lambda 1640$ profile is unshifted and has no redshifted emission (see Fig. 18a of Brandt et al. 1998). It can be added that unpublished thesis work by Cidale (1993) suggests that these same trends continue with emission in CIV. As a postulated hot temperature rise in these models is moved outward, a mild red emission component in CIV is enhanced while the absorption component remains almost the same. Some of our examples of observed variations below will illustrate this behavior.

The $\lambda 1640$ line has been interpreted by some authors to be stable in strength and thus to be a good measure of an O or early B star’s effective temperature. As detailed below, variability in this line has only seldom been reported in hot, chemically homogeneous, single stars. According to the VCR models, any variability of this line would require substantial changes in the star’s effective temperature, mass loss rate, or restructuring of the wind stratification. In cool stars $\lambda 1640$ variations arise from variable EUV irradiation in their chromospheres (Linsky et al. 1998). In this paper we will test several claims in the literature

for $\lambda 1640$ variability in Be star spectra and extend the search for this variability to a larger sample of B stars. Positive results of this search will be placed in the general context of the predictions of the VCR's ad hoc and nonstandard models of winds in hot stars.

2. Historical variations of He II $\lambda 1640$ in Be stars

VCR's models predict that $\lambda 1640$ variations are caused by dramatic changes in an O or B star's wind structure. This is consistent with the report by Peters (1990) that a weak correlation exists between the strength of the $\lambda 1640$ line and the wind component of CIV $\lambda 1550i$ of λ Eri (B2e). Peters noted that these variations depend in part on where the star is in its "wind oscillation cycle."

A second report of correlations between variations of He II and another line in a B star came from a campaign with a ground-based telescope and the *International Ultraviolet Explorer* (*IUE*) during three 8-h "shifts" on λ Eri. According to Smith et al. (1996), decreases in the $\lambda 1640$ and CIV resonance doublet absorptions coincided with the creation of a "dimple" on five occasions on 1990 October 21 and October 22 (see also Smith & Polidan 1993; Smith et al. 1996) in the line profile of $\lambda 6678$ and other optical He I lines¹. The timescale for these changes was as short as $\frac{1}{2}$ h. These line profile transients hint at the presence of rapid, possibly magnetic, activity close to the surface of the star. A connection with $\lambda 1640$ changes would further tie this activity to the photosphere. In view of this short history, we began our search for $\lambda 1640$ activity in spectra of early-type Be stars for which claims have been made preferentially for the presence of magnetic fields. Because the theoretical predictions are that changes in $\lambda 1640$ strength should be found in the dense, rapidly accelerating regions of winds of Be stars. It is logical to search the spectra of stars which have known histories of variable wind components of UV resonance lines.

3. Observations and data analysis

3.1. Reduction of *IUE* data

The ultraviolet data for these programs are extant high-dispersion *IUE* echellograms obtained through the large aperture of the Short Wavelength Prime (SWP) camera. These data were obtained from the MAST archive². An IDL program was written to read all spectra obtained for a star in the orders containing the echelle orders of $\lambda 1640$ and the resonance lines of CIV, NV, Si III, and Si IV. The spectra were cross correlated against one another to place them on a common wavelength scale an co-added. Small rescalings were then applied to the individual spectra to force their continua to the same level. Generally, these orders contain imprints of the instrumental calibration "re-seaux" etched onto the faceplates of the camera. The flux dips they cause are omitted in our plots to avoid possible confusion.

¹ Dimples are features appearing anywhere on the line profile (so far only for He I lines), described as central absorptions flanked by weak quasi-emission ones on either side that largely compensate the central absorption. These features typically have a lifetime of 2–3 h. Smith et al. (1996) reported that they may occur in the $\lambda 6678$ line of a few other Be stars.

² Multi-Mission Archive at Space Telescope Science Institute, in contract to the National Aeronautics and Space Administration.

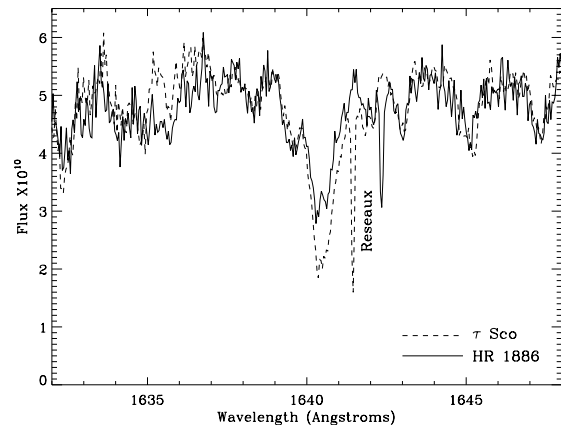


Fig. 1. High dispersion *IUE* spectra of the $\lambda 1640$ wavelength region of the sharp-lined stars τ Sco (B0.2 V) and HR 1886 (B1 V). The spectra partially resolve the He II 1640.4 Å line from the blend of Ni III/Fe II blend near 1640.0 Å. The wavelength range depicted corresponds approximately to the velocity range exhibited in most of the figures in this paper. The "Re-seaux" title notes the presence of a fiducial marker in the focal plane of the detector of the SWP camera.

3.2. Analysis of the $\lambda 1640$ spectral region

3.2.1. Dependences of the He II line and nearby blends

In order to study the He II $\lambda 1640$ line's behavior with respect to physical variables, we utilized the *SYNSPEC* line synthesis code (Hubeny et al. 1994) using LTE and non-LTE atmospheres for the effective temperature interval 21 000–29 000 K at $\log g = 4$ and for $\xi = 5 \text{ km s}^{-1}$. LTE models were taken from Kurucz (1993), while non-LTE models were taken from an extension of the OSTAR2002 grid for B stars (Lanz & Hubeny 2006). Although the $\lambda 1640$ line is an important transition complex in the He¹⁺ atom, its proximity in wavelength to several iron-group lines of comparable strength is one reason why it has been so little studied in B stars. The *SYNSPEC* program ameliorates this problem by permitting the user to identify the primary lines by eliminating candidates from the input line library and seeing if a feature of interest has disappeared in the recomputed spectrum. The program provides the ability to convolve the spectrum to mimic the effects of instrumental and rotational broadening. We utilized these functions to determine the contribution of the He II line to the aggregate " $\lambda 1640$ feature" as a function of stellar T_{eff} in spectra broadened by rotation.

To show why a spectral line synthesis approach is important to the study of $\lambda 1640$, we exhibit in Fig. 1 the wavelength region surrounding this line taken from *IUE* spectra of two B1 stars, τ Sco and HR 1886. The spectra of both stars are sharp-lined. As expected, we see that the He II line is stronger in τ Sco ($T_{\text{eff}} = 30\,200 \text{ K}$, $\log g = 4.2$; Hunter et al. 2005) than in HR 1886 ($T_{\text{eff}} = 23\,300 \text{ K}$, $\log g = 4.1$; Lyubimkov et al. 2005). The figure also shows that the absorptions of nearby lines must be included in the measurement of the total strength of " $\lambda 1640$ " in broad lined spectra. Our spectral line syntheses have enabled us to identify these blends as follows. Started from the blue edge of the aggregate, that the strong feature at 1639.4 Å is itself a blend of a Zn III ($\lambda 1639.42$) and an Fe line. The latter may be either Fe IV $\lambda 1640.40$ or Fe II $\lambda 1640.40$ for spectra of type B0 or B2, respectively. Dominating the blue half of the He II line is a feature at 1640.0 Å. For late O to B0.2-type stars, this feature is a blend of excited Fe IV lines at $\lambda 1640.04$ and $\lambda 1640.15$. For B1–B2 stars the composition of this blend has shifted to

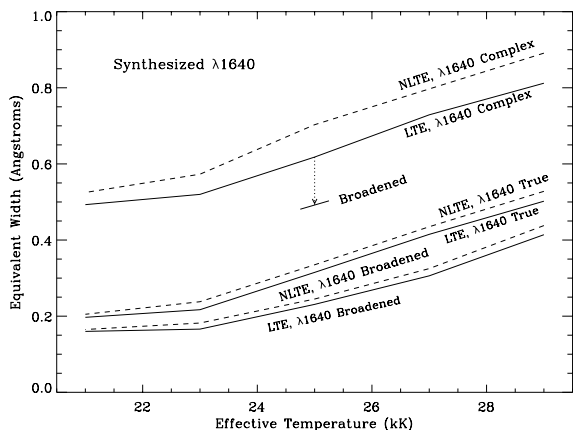


Fig. 2. The equivalent width contributions to the He II $\lambda 1640$ blend as a function of stellar effective temperature, computed from both LTE (solid line) and non-LTE (dashed) model atmospheres and measured over the wavelength interval $\lambda\lambda 1638.7\text{--}1641.5$. Pairs of solutions are shown for the unrotated and broadened ($V_{\text{rot}} \sin i = 300 \text{ km s}^{-1}$) profiles. The lower group of lines correspond to the equivalent widths found for the He II transitions alone. Normal compositions and a microturbulent velocity of 5 km s^{-1} are assumed.

Ni III $\lambda 1639.99$ and secondarily to Fe II $\lambda 1640.15$. Just to the red of the He II line, a strong blend of Fe IV $\lambda 1640.78$ line at type B0 gives way to a weak Fe II $\lambda 1640.86$ line.

The fractional contribution of the He II line within the $\lambda 1640$ feature, along with the dependence of the strength of the total aggregate, is plotted in Fig. 2. This figure depicts the equivalent width-temperature relations for three pairs of spectra computed with *SYNSPEC* for LTE and non-LTE atmospheres. In constructing the first (“True”) pair of models, we have removed all lines from metal ions from the input line library and computed the equivalent width between “continuum” points at 1638.7 \AA and 1641.5 \AA . This is almost identical to the wavelength interval selected by Peters (1990) for her measurements. Second, and beneath the “True” relations in Fig. 2, we show the relation for the same lines “spun up” to a rotational velocity of 300 km s^{-1} and measured according to the now lower “continuum” points in the same wavelength interval as in the first case. A third pair of equivalent relations is measured with the metal lines reinserted in the synthesized spectrum. The equivalent width for a fully broadened feature of the $\lambda 1640$ aggregate is shown for reference in the middle of the diagram for $T_{\text{eff}} = 25\,000 \text{ K}$. Altogether, Fig. 2 brings out several characteristics of the $\lambda 1640$ feature. First, all relations run roughly parallel to one another. Therefore, whichever relation one follows will undergo the same fractional change as one moves to a new effective temperature. For example, it is a remarkable coincidence that the blends to the blue and red of He II maintain their strengths relative to He II through the early B spectral types. Second, the loss of equivalent width from an undersetting of the continuum in a rotationally broadened spectrum is substantial, about 30%. This affirms the necessity of measuring the strengths of the $\lambda 1640$ aggregate in the same way for the range of stellar rotational velocities. Third, the contribution of the iron lines is almost half the strength of the total aggregate (for example, 0.30 \AA of the total of 0.62 \AA at $T_{\text{eff}} = 25\,000 \text{ K}$). Fourth, the enhancement of the line strength due to non-LTE effects is very small.

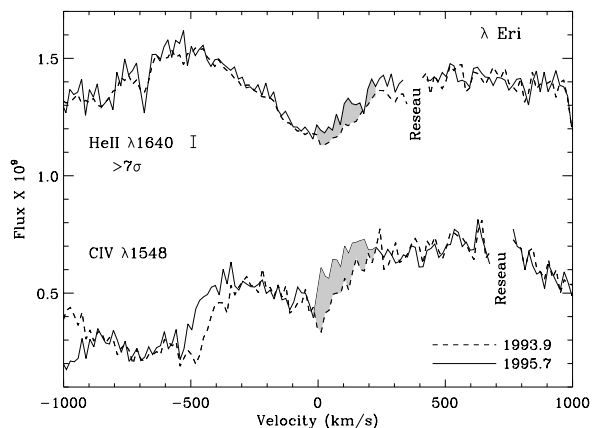


Fig. 3. *IUE* spectra of λ Eri obtained from observations during the epochs 1993.7–1994.1 and 1995.8 for the He II and Si IV doublet. The 1993–4 spectra are smoothed over 2 points in this plot. The shaded areas indicate the variations of the photospheric components; significance on He II is for this shaded area. In all plots, we assume a centroid wavelength 1640.3 for the $\lambda 1640$ aggregate feature. In this convention the He II feature centroid will correspond to a velocity of about $+55 \text{ km s}^{-1}$. Unless otherwise noted, the velocity system for the C IV doublet is referenced to the $\lambda 1550.8$ component.

3.2.2. Statistical analysis of the $\lambda 1640$ variations

In order to undertake a quantitative analysis of the $\lambda 1640$ variations, we first “conditioned” the data, that is we standardized the continuum levels and slopes (which changed over the *IUE* lifetime as the detector degraded) of the constituent spectra. We performed these steps by coadding all the spectra and choosing two generally line-free regions across the order containing the He II line and resonance doublets of interest. For this purpose we chose two velocity regions (relative to line center) at $-1200\text{--}700 \text{ km s}^{-1}$ and $+350\text{--}900 \text{ km s}^{-1}$. The blue window of each spectrum was scaled relative to the mean. The spectrum were then individually detrended relative to the mean again by an interactive computer routine (generally by $\leq 5\text{--}7\%$ from one end of our echelle order to the other). We then binned the spectra in wavelength by a ratio of 2 to 1 pixels, thus making the value of each binned pixel substantially independent of the values of its neighbors. Although in a few cases we have smoothed spectra for our plotting presentations, our statistical tests described below were performed on the unsmoothed data. To obtain an estimate of the rms noise level of our spectral comparisons shown in Figs. 3–21, we used the median of the absolute value of the differences of spectra in the quasi-continuum windows. The characteristic signal-to-noise ratios derived in this fashion were 20–27 per binned pixel for pairs of spectra, ~ 35 for comparisons of one spectrum against a seasonal average, and ~ 70 for averages of two seasons represented by large numbers of spectra.

To determine the statistical significances of our trial $\lambda 1640$ variations, we made the assumption that the data noise is gaussian. Veteran users of *IUE* data will recognize that this is formally a risky assumption for flux excursions of perhaps 2 rms or more. However, since most flux differences within the profile do not exceed $1\text{--}1\frac{1}{2}$ rms, the errors caused by this assumption are unlikely to be serious. We quantified the statistical significances, “ σ ”, of the line strength variations with a computer program we wrote that uses simple Monte Carlo approach. Our procedure was to define the wings of the entire profile and to use the rms level determined above to determine the statistical

Table 1. Relevant parameters for program Be stars (ordered by right ascension).

Name	HD Name	Sp.	Ref.	$V \sin i$	Ref.	T_{eff}	Ref.
λ Eri	HD 33328	B2 IVe	1	325	1	24 000	2
ψ^1 Ori	HD 35439	B1 Ve	3	305	1	25 400	3
ω Ori	HD 37490	B2e III	4	172	5	20 020	5
19 Mon	HD 52918	B1 IV	6	264	7	24 000	5
HR 3186	HD 67536	B2.5n(e)	8	292	9	20 000	10
μ Cen	HD 120324	B2 IVe	11	130	12	19 970	13
η Cen	HD 127972	B1.5 IVe	14	350	4	21 860	15
2 Vul	HD 180968	B1 IV	6	332	16	25 000	10
π Aqr	HD 212571	B1 Ve	6	250	17	25 000	17
6 Cep	HD 203467	B2.5e	18	150	18	20 000	10

Reference. 1: Abt (2002), 2: Hummel & Vrancken (2000), 3: Lamer & Waters (1987), 4: Slettebak (1982), 5: Neiner et al. (2003), 6: Lesh (1968), 7: Balona (2002), 8: Hanuschik et al. (1996), 9: Uesugi & Fukuda (1970), 10: this paper, 11: Hiltner et al. (1969), 12: Brown & Verschueren (1997), 13: Rivinius et al. (2001), 14: Levenhagen et al. (2003), 15: Stefl et al. (1995), 16: Balona (1995), 17: Miroshnichenko et al. (2002), 18: Slettebak (1994).

likelihood of random variations across the profile causing a difference in the absorption anywhere in the profile by at least the observed amount. Notice that this procedure estimates the significance level irrespective of “sympathetic” responses in the C IV or Si IV lines.

As an initial check on our technique, we compared the fluctuations of He II line profiles of the rapidly rotating B3 V star η UMa. The *IUE* satellite observed this star a total of 64 times with the SWP camera as a calibration standard during the interval 1978–1994. Using our Monte Carlo program, we searched for statistically significant line profile variations from the mean profile. We found fluctuations neither over the whole profile or the red or blue halves greater than 1.6 – 1.7σ . Moreover, in the instances of greatest fluctuations from the mean there were no sympathetic responses in the C IV or Si IV lines.

Because the “eye” is a good judge of sustained flux variations of several pixels, it is not surprising that we found the overwhelming number of candidate variations we initially selected turned out to be significant to at least the 3σ (0.13%) level. We relaxed this criterion only in Fig. 15, in which evidence from a simultaneous strong C IV variation in the same velocity range is overwhelming. Note also that our algorithm tests only changes in overall line strength. Thus, it is not an effective tool to measure the significance of high frequency variations of opposing signs across the profile. For this reason we withdrew two examples of possible “emission spikes” because they were not found to be statistically significant when tested against simulations over the whole line profile (typically $\pm 300 \text{ km s}^{-1}$). In several cases the line strength contribution in one region of the profile overwhelmed a variation of opposite sign in another and nevertheless was significant over the whole profile. For example, for Fig. 20 our annotated significances σ refer to the *net* difference of the opposing contributions. In two of our examples (Figs. 9 and 10) opposite contributions of two segments of the line profile are about equal. In these cases we will give the significances for the corresponding halves of the profiles. Overall, it is likely that our procedures have excluded several true variations of marginal significances.

3.3. Selection of $\lambda 1640$ -variable Be stars

The impetus for this program was the example of $\lambda 1640$ variations in the B2e star λ Eri and μ Cen. As discussed below, $\lambda 1640$ and various optical He I lines in the spectra of these two stars undergo rapid activity. This fact has led several authors to

suggest that magnetic fields play a role in this activity. Recently, Neiner et al. (2003) have reported the detection of a rotationally modulated magnetic signature in ω Ori. Thus, we will start our survey of He II line variability by discussing these three stars. Various authors (e.g., ten Hulve 2004) have suggested that magnetic fields play a role in aperiodic variability of the photospheric components of the C IV and other resonance lines. We will therefore treat these stars as well.

To extend the search for He II line variability further, we surveyed all B0–B2.5 Be stars that the *IUE* observed at high dispersion through the large aperture of the SWP camera at least 10 times. This search netted a sample of 74 stars. To this number we also added several early-Bn stars, such as η UMa, that were observed many times, but none of them exhibited He II line variations. Likewise, we note that some Bp stars exhibit variations in $\lambda 1640$ because of their heterogeneous He surface abundances (Bp stars such as σ Ori E), and these are not included in our program. Our search is admitted not exhaustive, and it may contain selection biases. However, note that rotational velocity was not a search criterion, except implicitly through our choice of Be stars.

Table 1 lists 10 program stars for which we have found variable He II lines, representing a data sample of 558 *IUE* SWP-camera echellograms. The table also gives spectral types, $V \sin i$, and T_{eff} values according to the cited references. We have given preference to spectral types determined at high resolution and for velocities and temperatures to determinations by recent authors. Rough estimates of T_{eff} for HD 67536, 2 Vul, and 6 Cep are based on the observed He II line strength, but these were not used in this work.

4. Results

4.1. Magnetic candidates: λ Eri, ω CMa, and μ Cen

4.1.1. λ Eridani

λ Eri is a rapidly rotating B2 IVe star that has been studied extensively in the optical, UV, and X-ray wavelength ranges. Searches for velocity variations have produced no evidence that the star is in a binary (Bolton 1982; Smith 1989). Since the discovery of H α emission in this star by Irvine (1975), this line has been observed to cycle between emission and absorption states. Bolton (1982) first reported that the star to be a periodic velocity variable. These variations are now generally recognized to be due to nonradial pulsations (NRP; e.g., Rivinius et al. 2003,

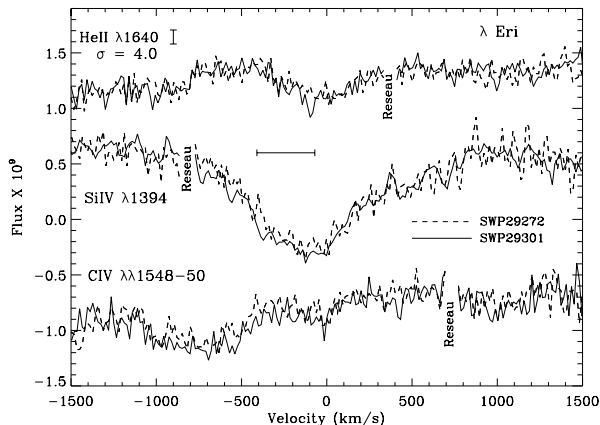


Fig. 4. Comparison of *IUE* observations SWP 29272 and 29301 (2.0 days later) on λ Eri for He II, Si IV $\lambda 1394$ line and the C IV doublet in the spectra. The comb indicates the velocity range over which there are correlated variations.

but cf. Balona & James 2002). The star’s broad spectral lines have prevented the direct detection of a magnetic field. However, magnetic activity might explain several types of activity. The first example of this, “dimples”, has been noted already. Second, Smith (2000) has noted the occasional presence of “high velocity absorptions” in the He I $\lambda 6678$ profiles. These events last several hours and have been interpreted as ejections of blobs, many of which return to the star (Smith et al. 1991; Smith 2000; see also μ Cen discussion). A third possible case for magnetic activity is the observation of “flows” across the He I $\lambda 6678$ line profile over several hours (Smith 1989). This suggests that the matter is channeled along prominence-like structures over the star’s surface. A fourth example is the observation by the *Rosat* satellite of a strong soft X-ray flare, lasting several hours (Smith et al. 1993). Groote & Schmitt (2004) have pointed to the similarity of this event and a flare observed in the magnetic Bp star, σ Ori, E.

Evidence also exists for a periodicity or cyclicity of ≈ 475 days for the star’s “Be outbursts” (Mennickent et al. 1998; Balona & James 2002). Several observers (e.g., Peters 1990) have also reported increases in H α emission strength, and the appearance of Discrete Absorption Components (DACs) of the C IV and Si IV resonance doublets at about -900 km s $^{-1}$.

We found variations over both short and long timescales in our examination of the He II $\lambda 1640$ line of λ Eri in the *IUE* archives. As a start, we note that the He II line equivalent widths decreased substantially, and with almost no overlap between their respective ranges between the epochs 1993.79–1994.06 and 1995.7. A comparison of the mean profiles during these times is depicted in Fig. 3. This plot shows that the He II line is either partially filled in on the red side (0 to $+300$ km s $^{-1}$), or Doppler shifted to to the blue. This interpretational ambiguity is decisively settled by the filling in of the red wing of the C IV doublet at 0 – 240 km s $^{-1}$ in this figure. A similar difference is found in the Si IV doublet (not shown).

The *MAST/IUE* archive contains 145 SWP high-dispersion observations of λ Eri distributed over a large range of timescales, including monitoring campaigns in 1982 and 1996. We have found rapid variations of the He, II, Si IV and C IV lines during these times. Figures 4 and 5 document changes over the central region of the photospheric profile. The intervals between these two pairs of observations are 48 and 19 h, respectively. Figure 5 is especially interesting because it compares the profiles during

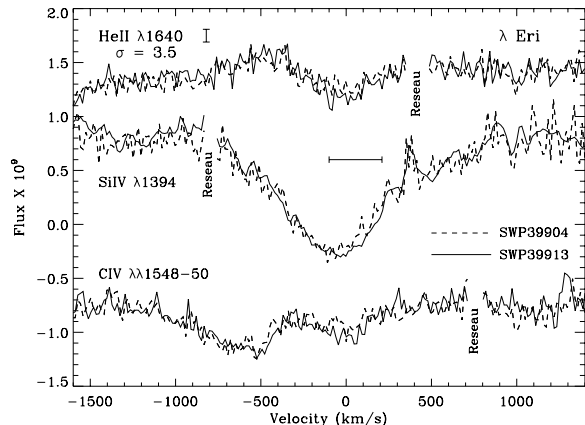


Fig. 5. Comparison of *IUE* observations SWP 39904 and 39911 (19 h later) for He II, the C IV doublet and the Si IV $\lambda 1394$ line in λ Eri. This figure shows typical rapid weakenings of the He II line in this star.

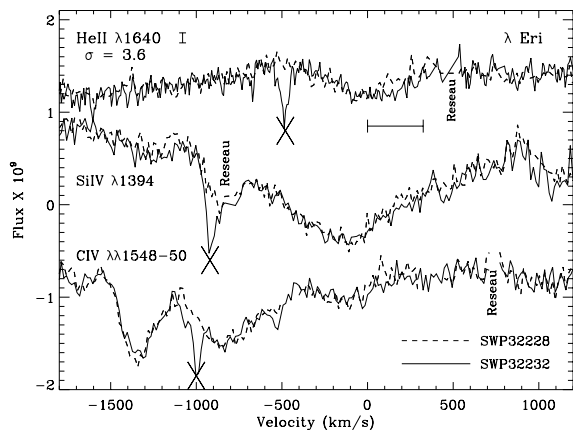


Fig. 6. Comparison of *IUE* observations SWP 32228 and 32232 (3.9 h later) for the He II, the C IV, and Si IV $\lambda 1394$ lines in λ Eri. This figure shows typical rapid filling in of the red wing of the He II line in this star. The X-marked features in all three features are instrumental (“missing minor frames”).

a pair of dimple-active and -inactive states (Smith et al. 1996; see Figs. 5 and 6). As opposed to the He I lines, the He II respond to dimples by small *weakenings*. In Fig. 6 we show variations over 4-h in the red wings of the He II, C IV and Si IV $\lambda 1394$ lines. Because the increased flux may not exceed the continuum level, we do not know if this is due to emission or to a weakening of absorption.

4.1.2. ω Orionis

ω Ori is a typical B2e star that seems to oscillate between B-normal and Be H α emission states. So far, these oscillations seem to be cyclical rather than strictly periodic. The high-velocity (wind) components of the resonance lines often exhibit large changes. The profiles are relatively narrow for a classical Be star. This fact has permitted the discovery of a weak dipolar surface magnetic field that modulates on a rotational period of 1.29 days (Neiner et al. 2003). Given the expected radius of a B2 main sequence star, this period implies that we view this star from an intermediate aspect. Neiner et al. (2003) also reported an enhancement of nitrogen from an optical line. C IV variations inform us that the wind of this star can be variable on timescales as short as $1\frac{1}{2}$ h. Such variations suggest

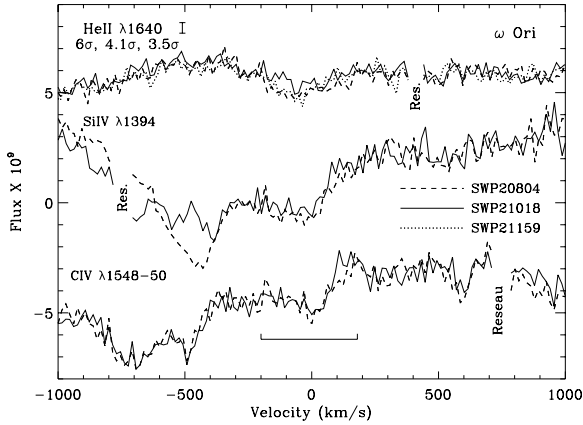


Fig. 7. IUE observations of ω Ori during 1983 that show variations of the He II, Si IV and C IV lines. The interval between the solid and dashed line observations is 16 days. The dotted line (He II only) shows the observation SWP21159 13 days after the second observation. The significances quoted is for differences between the first and second, second and third, and first and third He II observations, respectively.

that localized and hence anisotropic changes in the wind in the rapidly accelerating zone occur close to the star (Sonneborn et al. 1988).

The IUE archive includes 189 SWP high-resolution observations of ω Ori. Of these, 110 are included during intensive campaigns in 1982 and 1996 and intermittent monitoring in 1983. According to ground-based polarization studies, the star underwent a strong, rapidly evolving outburst in 1983 (Sonneborn et al. 1983). This event was accompanied by the emergence of even stronger DACs in the C IV lines, though these were shifted to lower velocities. The star's $H\alpha$ line was in strong emission in December, 1996, and by 1999 its equal V , R emissions were still unchanged (Peters 2005). Thus, it is likely that when the 1996 campaign was conducted, ω Ori was likewise in a Be active state. Although the star's $H\alpha$ line showed strong emission during the 1982–3 episode, there are apparently no published accounts of its status during early 1996. However, Neiner et al. (2003) documented that the emission was moderately strong in 1998 and declining through 1999. For completeness, we note that the 1996 spectra of ω Ori exhibit stronger NV doublet absorptions than during 1982. This is among the few cases in our study for which we could find a correlation between these He II and NV temperature indicators. The difficulty of seeing the correlation for other stars is mainly due to the weakness of NV lines in their spectra.

We found several examples of rapid and long-term variability in the He II line variability for this star. Starting again with the long-variations, we noticed systematic differences in the mean photospheric profile strengths for 1982 and 1996 observations. The 1982 profiles exhibit a filling in of the red wing and a tapered blue absorption wing. The variations in the He II line of ω Ori are not always replicated in the C IV and Si IV doublet lines, even though the doublets show substantial *inter alia* variations at high velocities.

Sonneborn et al. (1988) discussed the wind activity in this star during 1982–3. Figure 7 exhibits one observation, SWP21018, discussed in their paper and another obtained 16 days earlier. During this time the He II profile showed substantial activity over sometimes broad, and at other times narrow, wavelength ranges. The Si IV and C IV doublets exhibited apparent incipient emission fluctuations in their red wings during these times. In the blue/central parts of the line, the Si IV doublet changed very little and the C IV lines not at all. Some

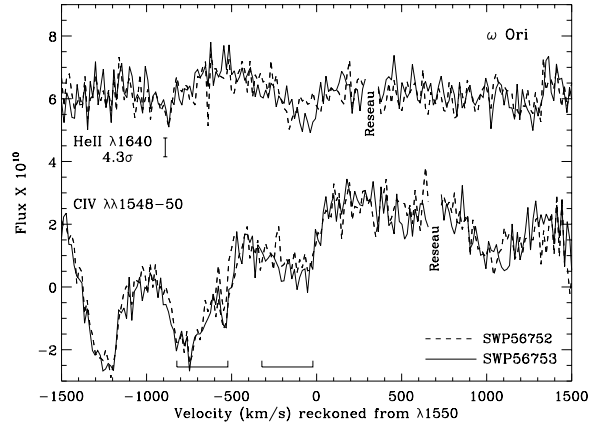


Fig. 8. IUE observations of ω Ori over a 12 h interval in 1983, exhibiting variations of the He II, Si IV and C IV lines. Errors on He II are taken in the interval 0–350 km s⁻¹.

13 days later, the He II line shows the same filling in on the red side as for SWP21018, but the blue side of the line again shows full-strength absorption. An important interpretation from these comparisons of He II and resonance line variations is that changes observed at the base of the wind do not necessarily correlate well with those further out in the flow.

These lines also exhibit variations on a rapid timescale of 12 h; see Fig. 8. In this case the central core of $\lambda 1640$ (solid line) has deepened while the red wing has filled in. The C IV doublet shows an overall weakening over the whole photospheric components. The Si IV lines exhibit no change. We speculate that because ω Ori has a magnetic field, these rapid variations might arise from dissipative magnetic processes in the outer atmosphere.

4.2. Stars with possible $\lambda 1640$ red wing emission

4.2.1. μ Centauri

This B2e star has been extensively observed and shows a rich activity in its light curve, $H\alpha$, and other spectral lines. The light curve undergoes sporadic brightenings of up a few tenths of a magnitude (Baade et al. 2001) for reasons unknown. The $H\alpha$ emission component exhibits activity episodes over a variety of amplitudes and timescales (e.g., Hanuschik et al. 1993). The star's spectral lines are sharp, suggesting that it is viewed at a low inclination. μ Cen has been extensively monitored spectroscopically. Rivinius et al. (1998b) reported that its line profile variability can be decomposed into six nonradial pulsation periods. These modes cluster at 0.51 and 0.28 days. Rivinius et al. (1998a) have attempted to interpret the Be outburst in this star as an outcome of nonlinearities associated with the beating of these modes. In addition to activity associated with intermodal beating, aperiodic activity also appears to be present. Peters (1984b) noted that an optical He I line exhibited a rapidly appearing absorptions at velocities outside the photospheric profile over several minutes. Such transients, since dubbed “high velocity absorptions” seem to represent discrete ejections of blobs (Rivinius et al. 1998). Peters (1998) has also documented evidence of rapid, large-amplitude emission variations along the $\lambda 6678$ profile over several hours, suggesting that matter is channeled in arc-line prominences.

In our survey of the 34 available SWP echellograms for μ Cen, we found several variations of the $\lambda 1640$ line. This included a narrowing of the He II, Si III, Si IV, and Al III lines from

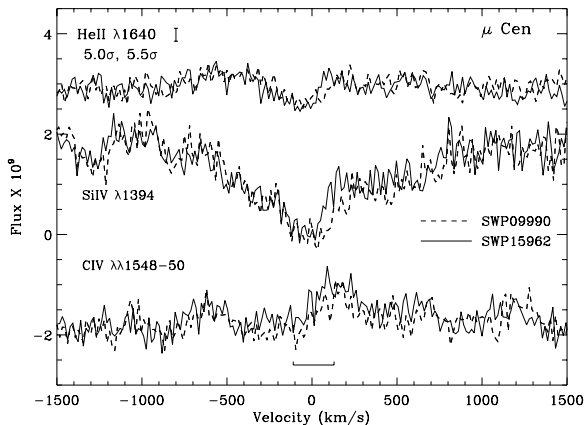


Fig. 9. A comparison of μ Cen’s He II and C IV lines in 1980 and 1982 for μ Cen. Note the weak red wing emission. Errors on He II refer to blue and red halves of the profile, respectively.

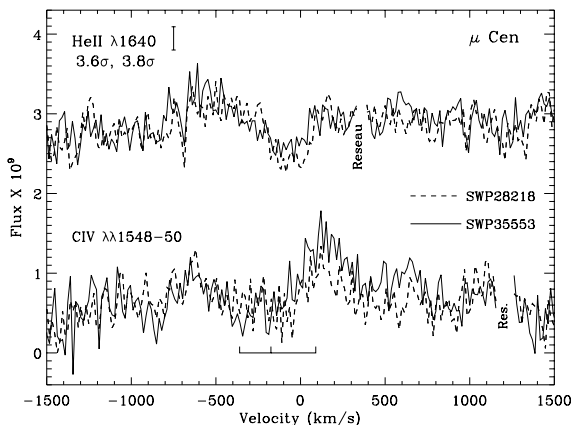


Fig. 10. A comparison of the He II and the C IV lines for the interval April 1986–February 1989 for μ Cen. Note the weakening of the He II line coincident with the formation of red wing emission in C IV. Errors on He II refer to blue/central and red portions of profile (see comb).

September 1980 to February 1981 reported by Peters (1984a). However, whereas Peters interpreted these differences in terms of line broadening during an $H\alpha$ emission episode, we believe these differences should be interpreted as a weakening of absorption and emergence of P Cygni emission component during the *later epoch*, making the profiles appear narrow. These differences can be seen in Fig. 9. Any possible doubt that the faint bump in the red wing of the C IV doublet are emission in this figure is dispelled by its behavior in Fig. 10. This plot compares observations of the He II and C IV lines made in 1989 and 1996. The 1989 profiles are weak and narrow. Although there is much activity in the red wings, the photospheric components of C IV show no variations. Just as for λ Eri and ω Ori, we were surprised to find that relatively large variations in the He II line of μ Cen can occur on short as well as long timescales. Although we have found convincing evidence for at least four cases in the He II line, residual red wing emission is actually more common for the C IV and Si IV doublets (Fig. 9). Moreover, short-term variations can occur in resonance lines of less excited ions like Si III and Al III (Peters 1984a). This suggests that the region of the wind affected extends further downstream than is the typical for other stars in our sample.

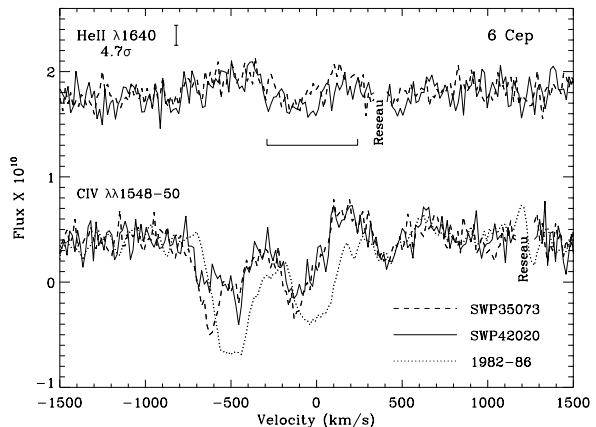


Fig. 11. A comparison 6 Cep’s He II and C IV lines for epochs 1989.0 and 1990.5. Note the inactivity of the red wing emission in the C IV line. The wind was in a different state during 1982–86 (C IV, dotted line).

4.2.2. 6 Cephei

Like μ Cen, 6 Cep is a B2.5e star with unusually narrow spectral lines for a Be star. Pavlovski et al. (1997) monitored the star’s optical flux but were unable to find optical continuum variations. In contrast, both its optical and UV spectrum are variable. The C IV resonance lines exhibit strong variations during oscillations of its wind state (e.g., Barker & Marlborough 1985; Grady et al. 1987; “GBS”). Abraham et al. (1993) have speculated that the star’s wind is responsible for the creation of a “stellar wind bubble”, which they were able to image with the *IRAS* satellite. Koubisky et al. (2005) have found a period of 1.621 days in the optical line profiles of 6 Cep. These authors believed that they could be attributed either to nonradial pulsations or a corotating disturbance or cloud over the star. However, we favor the pulsation alternative because in our present study we can see variations in lines arising from moderately excited excitation states, as would be expected in the photosphere.

The *IUE* archive contains 34 SWP echellograms of 6 Cep. From our inspection, we suspect that a few profiles undergo small amplitude variations. However, our statistical tests of these disclosed that only one was significant. A comparison of He II and the C IV doublet is shown in Fig. 11 for a pair of observations taken in 1989 and 1990. In this example, the He II line shows a general weakening of the photospheric profile and a distinctly raised red wing. The corresponding profile of the C IV doublet is consistent with true emission: its red wing is raised above the continuum level. Although the red wings of the C IV exhibit no changes during this time, the profiles develop a narrow absorption at about -150 km s^{-1} . This is just one of a few examples shown in the present paper of different types of simultaneous variations of He II and C IV. The example in Fig. 11 also adheres to our more general finding that a filling in of red wing emission in the He II line tends to accompany strong absorption at low negative velocity in the C IV doublet. To give some perspective as to how these C IV profiles differ from the “norm”, we exhibit in Fig. 11 the profiles of both pairs of observations from 1989 and 1990 and the mean profile for 1982–6 (dotted line).

4.2.3. HD 67536

HD 67536 is a somewhat understudied variable B2.5–B3n star. On some occasions its Balmer lines show emission (Hanuschik 1996). The structure and significant variability of its C IV lines is

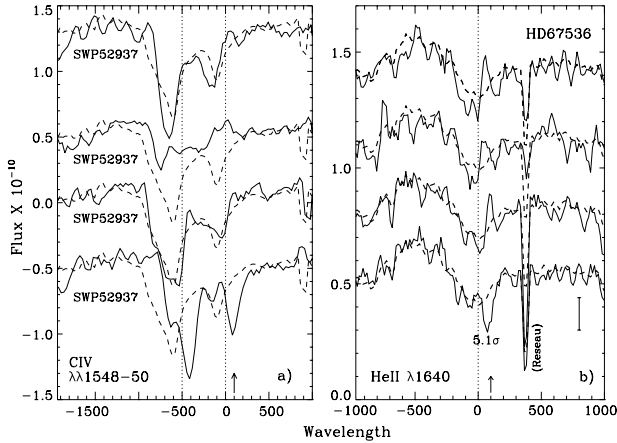


Fig. 12. A montage of four variations of the CIV and He II lines in 1983, 1986, 1994.7, and 1994.9 for HD 67536. The dashed line represents the mean of the available 22 spectra. The photospheric components of the CIV doublet of observation SWP 27503 (bold line) are nearly completely filled in. The average spectra (dashed plot) are binned to 4 instead of 2 pixels. Note the slightly sharp, red displaced features (in the first three cases in emission) in these lines. “ 5.1σ ” (panel b, fourth spectrum) refers only to the variation of the sharp absorption.

similar to that found in 6 Cep (GBS). Using this star as a prototype, ten Hulve (2004) and Henrichs et al. (2005) have identified a class of “magnetic” candidates based on the presence of variability between the rotational velocity limits $\pm V \sin i$ in the line profiles of this doublet. This working definition is reminiscent of the characteristic periodic absorption/emission behavior of these lines noted by Shore and colleagues (e.g., Shore & Brown 1990). However, the datasets for most or all of the 24 Be stars so characterized are too sparse to determine whether these variations are periodic.

In examining the 22 available *IUE* SWP echellograms for HD 67536, we found that variations at velocities above -600 km s^{-1} are readily apparent in the CIV and Si IV lines. Figure 12 exhibits four spectra obtained at epochs 1983, 1986, 1994.7, and 1994.9 along with the mean of all observations. Interestingly, the He II profiles in the first three exposures have a P Cygni-like character, which includes a narrow emission spike at about $+100 \text{ km s}^{-1}$. (Because the profile variations are so complicated we have not attempted to determine their statistical significances.) The CIV lines also show arguably weak emission at this velocity. Indeed in the SWP 27503 observation the doublet components are almost completely filled in out to the DAC at -300 km s^{-1} . Incidentally, this peculiar phenomenon cannot be explained by small changes in the T_{eff} over the whole stellar surface because the iron-group lines seem unaffected. Judging from previous exposures, the CIV line spectrum was in this filled-in state for at least 4 days when SWP 27503 was recorded. In the fourth example, depicted in Fig. 12, an observation taken in 1995.1, a narrow absorption appears, again at $+100 \text{ km s}^{-1}$, in CIV and He II lines. We not know if it is significant that each of these events occurs at nearly the same velocity.

4.3. Stars with $\lambda 1640$ blue-wing absorption

In contrast to the previous Be stars, spectra in the second half of our sample exhibit variations that are usually correlated with blue wing variations in CIV and/or Si IV, and occasionally even Si III resonance lines.

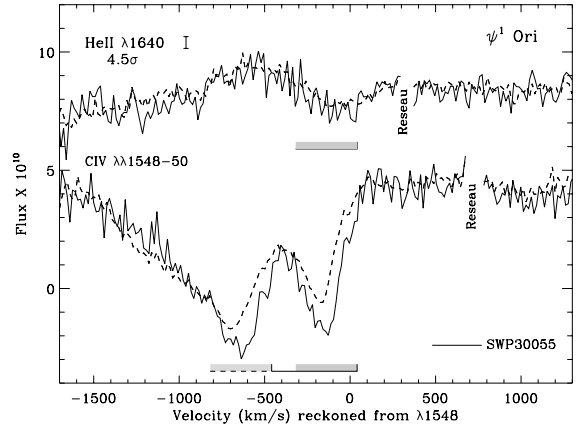


Fig. 13. The comparison of the stronger than unusual He II and CIV spectra for ψ^1 Ori obtained at 1987.2 relative to mean profiles.

4.3.1. ψ^1 Orionis

ψ^1 Ori is in many ways a typical early-type Be star. The spectral temperature diagnostics, including $\lambda 1640$ and resonance line wind features, are consistent with this classification. Like many other Be stars, it exhibits cyclic $H\alpha$ emission episodes. This emission was strong during the late 1970’s and early 1980’s (Barker 1983) when Lamers & Waters (1987) estimated the mass loss of ψ^1 Ori to lie in the range 10^{-8} – $4 \times 10^{-7} M_{\odot} \text{ yr}^{-1}$ from *Copernicus*, *IUE*, and *IRAS* data. This is among the highest mass loss rate range noted in these authors’ sample.

The *IUE* archive contain 26 SWP camera observations of this star. These are well enough distributed to give a sense of both rapid and long-term variations. From these data we found no evidence of rapid variability. Even over the long term, the fluctuations of this line are small compared to the moderate amplitudes of CIV activity. These variations extend over all possible velocities. Curiously, a strong “DAC-like” feature is present in the CIV complex at about -200 km s^{-1} in all the observations.

The He II variations in ψ^1 Ori seem to bridge the red-central profile activity seen in the examples discussed above and for the remaining stars in our sample. Up until the spectra of this star, we have not encountered He II variations in the blue wing. In fact, our first example, depicted in Fig. 13, exhibits an increased absorption over the range $+50$ to -300 km s^{-1} . The CIV lines show a similar variation in their blue wings, but they also exhibit a weakening at high velocities of -1000 to -1500 km s^{-1} . Figure 14 exhibits a second example of He II variability. On this occasion absorptions are present, a narrow feature at $+100 \text{ km s}^{-1}$ and a broad one in the blue wing. The narrow but not the broad feature is present in the corresponding CIV observation.

4.3.2. η Centauri

A rapidly rotating B2e star, η Cen has been the subject of much recent study. Its optical and UV lines and UV continuum undergo regular short-term variations with a dominant period near 0.64 days (Leister et al. 1995; Steffl et al. 1995; Peters & Gies 2000). In addition, the star’s $H\alpha$ line exhibits strong oscillations over long timescales (Dachs et al. 1986). Rivinius (2005) has suggested that the star ejects blobs that develop into ring-like structures.

Inspection of the CIV lines discloses considerable “slow” variability in the range -1500 to $\sim +200 \text{ km s}^{-1}$. The line cores

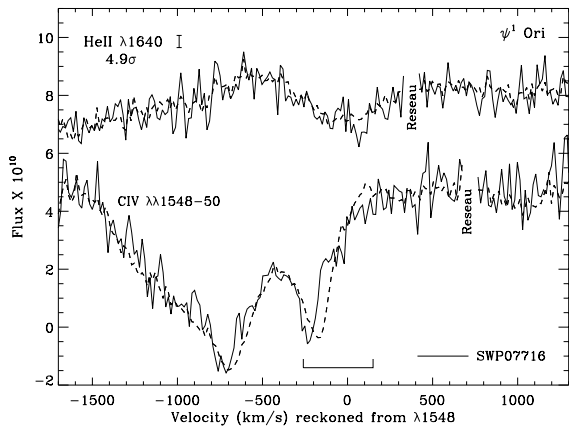


Fig. 14. A comparison of the He II and CIV spectra for ψ^1 Ori at the epoch 1980.0 relative to the mean profiles. The single spectrum shows a weak sharp absorption feature at 100 km s^{-1} .

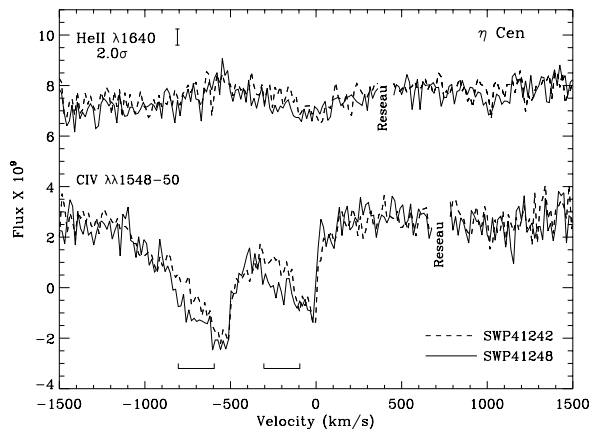


Fig. 15. A comparison of the He II and CIV spectra during the 1991.2 campaign on η Cen. Notice the variation of the blue wings over over a 7.4 h interval. Our significance acceptance criterion was relaxed in this one case because of the correlation with the strong CIV variation.

show a peculiar double-lobed structure, and the core centroid positions vary between -50 and -250 km s^{-1} . Although the red wings of the CIV doublet are typically filled in by emission, the changes in their profiles are small. To a lesser extent, these statements also apply to the Si IV doublet and even the Si III $\lambda 1206$ line.

The *IUE* obtained 28 *SWP* echellograms of this star from 1983 through 1991. These were roughly evenly distributed between two observing campaigns during each epoch. The He II line shows correlated variations with CIV in several instances. First, we noticed long-term differences in the sense that the wings of both lines were more depressed in 1991. Rapid variability is also evident, and we display two examples. Figure 15 exhibits variations in these lines over the same velocity range and over an interval of 7.4 h. During this time the He II line and the CIV doublet developed a low-velocity absorption at about -200 km s^{-1} . Figure 16 shows a weakening of emission over an interval of 7 h. Taken together, these two examples are the only cases we have of activity in the blue and red wing of $\lambda 1640$ line over a time interval that is not much longer than the star's rotational period (1.5 days).

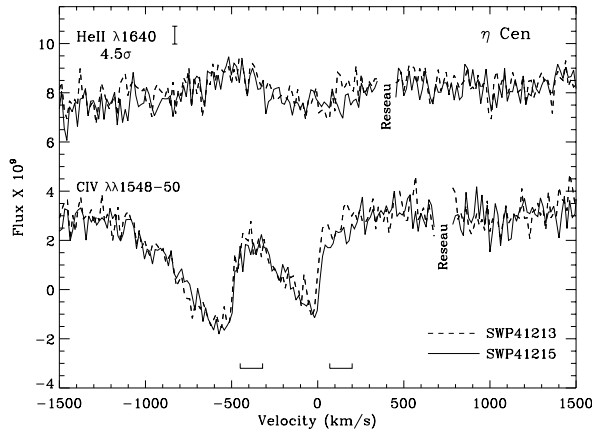


Fig. 16. A comparison of the He II and CIV lines during the 1991.2 campaign on η Cen. Note the variation of the red wings over a 3.9 h interval.

4.3.3. π Aquarii

π Aqr is an active B1e star and is also a double-lined, 84-day spectroscopic binary. The component mass ratio is 0.16, which implies that the secondary is an early-type A star (Bjorkman et al. 2002). Detailed fits of the H α emission profiles suggest that we view this star at a high inclination, i.e., $i \approx 70^\circ$ (Hanuschik et al. 1996). The X-ray flux of this star is high for a Be star, indeed about one half that of the X-ray anomalous Be star γ Cas. Also, unusually for a Be star, high energy emission has been detected by the *EUVE* satellite (Christian et al. 1999). Moreover, its IR flux is quite variable, even for a Be star. Bjorkman et al. have suggested that the star's variable H α emission can be used to measure a time-dependent mass transfer from the secondary star on to the Be star's disk. (This assumes that the disk is formed by binary accretion and not by decretion, as is ordinary for Be stars.) The abnormal absorption strength of the He I $\lambda 5876$ is consistent with the formation of part of this line close to the Be star's surface, perhaps in the inner region of the disk.

The *IUE* observed π Aqr 23 times during 1978–9 and 1985–91 with the *SWP* camera. Unusually for a Be star, the NV doublet is not only present but strikingly variable. Ringuet et al. (1981) have reported emission in these lines, and we attribute this to mass transfer from the companion to the Be star. The resonance lines of CIV, Si IV, and Si III exhibit a characteristic range and type of variability for an active Be star. Moreover, because its measured mass loss rate of $\approx 2.5 \times 10^{-9} M_\odot \text{ yr}^{-1}$ (Freitas Pacheco 1982; Snow 1981) is typical for a Be star, we believe that the variable blue wings of these lines are due to fluctuations in the Be star's wind. It remains to be added that the Be star's optical lines reveal the presence of traveling bumps due to a 1.88 h oscillation (Peters & Gies 2005; the grayscale in this paper offers an unusually clear depiction of the increased acceleration of NRP bumps at the edges of the line profile).

This star's He II line exhibits remarkable blue-wing strengthenings which track strengthenings of the strong blue wings of the CIV and Si IV doublets. Figure 17 exhibits the variation of these lines during epochs 1979.5 and 1979.8. Although not plotted, the Si III $\lambda 1206$ line shows the same enhanced absorption out to a common edge of $\sim -1300 \text{ km s}^{-1}$. In Fig. 17 the blue wing of the He II line is enhanced out to -500 km s^{-1} . Likewise, Fig. 18 exhibits both a blue wing strengthening red wing weakening in 1993.9 relative to 1979.5. The Si III and Si IV resonance lines show similar variations as CIV over the intervals covered in our two figures. Because the statistical tool we described in

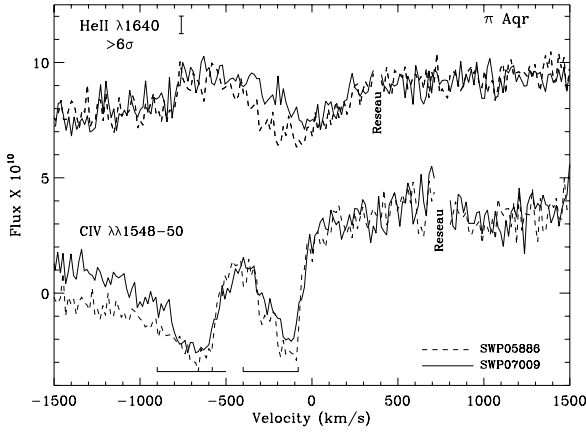


Fig. 17. A comparison of the He II and CIV spectra between epochs 1979.5 and 1979.8 for π Aqr.

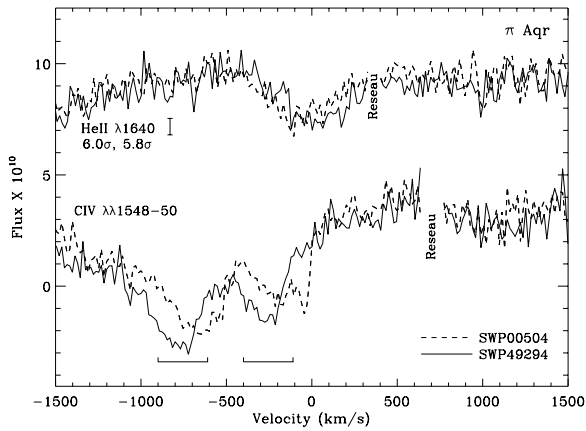


Fig. 18. A comparison of the He II and CIV spectra between epochs 1988.4 and 1993.9 for π Aqr. Errors on He II are given for the blue wing (comb interval) and red wing, respectively.

Sect. 3.2.2 evaluates changes for a chosen wavelength interval, we exhibit the significance of our test for just the low negative velocities of He II defined by the comb symbol.

4.3.4. 2 Vulpeculae

Although 2 Vul has not been classified as a Be star, we included it in our sample because Zaal et al. (1997) had detected emission in its near-infrared Brackett hydrogen lines. This emission implies the presence of a thin disk. Although Percy et al. (1988) have reported that this star has a photometric period near 0.61 days, Balona (1995) found a period of 1.27 days. Hanula & Gies (1994) discovered regular line profile variations, suggesting that these variations are due to nonradial pulsation. Prinja (1989) has determined a mass loss rate of $1 \times 10^{-9} M_{\odot} \text{ yr}^{-1}$ from resonance lines of several ions.

The *IUE* archive includes 39 *SWP* observations, of which 19 were recorded in a campaign at 1992.7. GBS and ten Hulve (2004) found that the CIV lines are variable. Ten Hulve considered it a “magnetic star”. The mean CIV profiles are extremely strong, indeed so much so that the two components merge into a single broad trough with a minimum at $\sim -400 \text{ km s}^{-1}$. Occasionally, the small-scale variations take the form of narrow *emissions* centered at a few high velocities along the profile. In this sense the resonance lines are more characteristic of an active O star than a Be star.

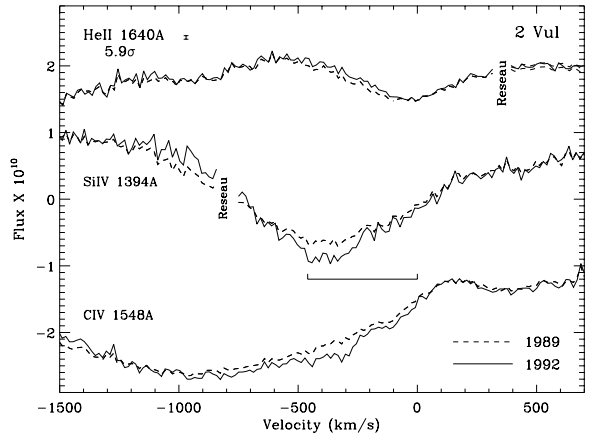


Fig. 19. A comparison of the He II, CIV, and Si IV $\lambda 1394$ line spectra between epochs 1989 (SWP 36329) and 1992 for 2 Vul. The comb shows the region of differences of the profiles, which are also shared by the Si III $\lambda 1206$ line (not shown).

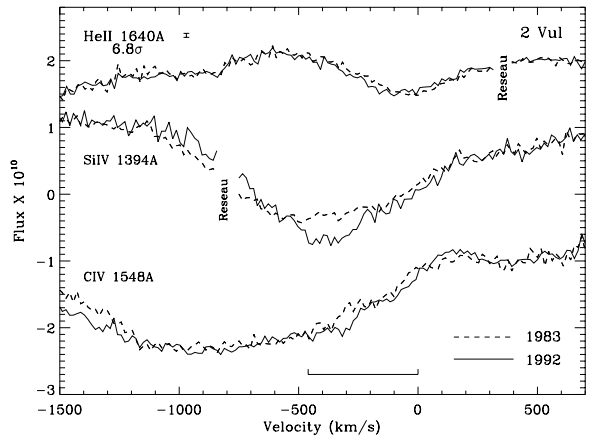


Fig. 20. A comparison of the He II, CIV, and Si IV $\lambda 1394$ spectra for 2 Vul for the epochs 1983 and 1992. Although not shown, the Si III line exhibits similar variations.

Rapid He II variations are not discernible in the *IUE* spectra of this star. We have selected two examples of long-term variability. Figure 19 shows that a difference in the profiles of He II, the CIV doublet, and Si IV $\lambda 1394$ between an observation in 1989 and the epochal average for 1992. It is clear that the wind was far stronger during the latter epoch and produced enhanced absorption out to -1200 km s^{-1} . The behavior of the Si III $\lambda 1206$ line, not shown, is similar to Si IV. This fact suggests that the variations are due to large increases in mass rather than a shift in wind ionization. In contrast, the DAC in the Si III profile is centered only at -800 km s^{-1} , indicating that the position of this feature is governed by wind ionization. The blue wing of the He II line is uniformly stronger in 1989 than 1992 and extends to -400 km s^{-1} .

Our second example of $\lambda 1640$ variability is shown in Fig. 20. This figure compares the behavior of He II, CIV, and Si IV lines between 1983 and 1992. This contrast is smaller than the previous one with respect to 1989. The CIV, Si IV, and Si III (not shown) lines show variations in an opposite sense from He II – for example, in the range -700 to -1000 km s^{-1} . This suggests that ionization shifts are at play in this case. The strengthening of the blue wing of the He II line is small but consistent out to at least -500 km s^{-1} . Although this slow change occurs along

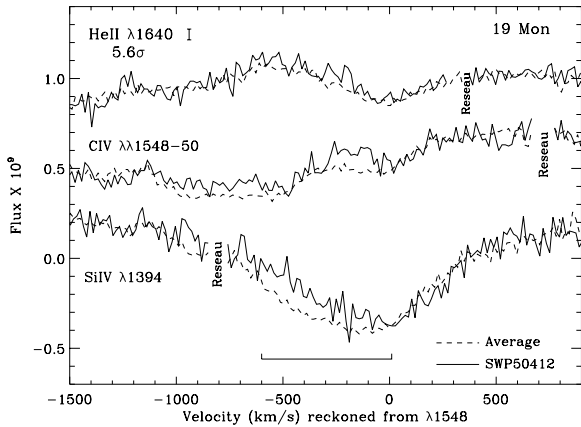


Fig. 21. A comparison of the He II, C IV, and Si IV $\lambda 1394$ spectra for a mean and an observation of 19 Mon during 1994.2. The significance on He II refers to the *whole profile*. Thus, the significance of the variation of the blue wing exceeds 6.0σ .

the photospheric profile too, this is another case in which the blue-shifted absorption is formed in the wind.

4.3.5. 19 Monocerotis

19 Mon, the final star for which we found $\lambda 1640$ variability, is also a rapidly rotating B1e star near the main sequence. It exhibits at least two large-amplitude prograde nonradial pulsations with periods near 5 h (Balona et al. 2002). Although the star’s Be type is based on emission twice detected at low dispersion, Balona et al. have disputed whether the $H\alpha$ line really has ever displayed emission. However, GBS and ten Hulle (2004) have noted the variations of its C IV lines. Ten Hulle considered this another example of a “magnetic star”. For this reason, we are inclined to believe the original spectroscopic emission reports and have included 19 Mon in our Be star sample.

Figure 21 exhibits the only possible example of a likely deviation of the He II line from its mean profile from the 15 available *IUE* spectra. The diminished absorption in this observation (SWP50412) begins at line center and extends out to -700 km s^{-1} . Remarkably, this variation is anticorrelated with the C IV and Si IV strengthenings. Yet, it appears once again that the He II formation region extends into the wind.

5. Discussion

5.1. Characterization of the variability

The He II $\lambda 1640$ variations we have found fall into one of the following patterns:

- The line preferentially fills in on the red side (λ Eri, μ Cen, 6 Cep, and η Cen; e.g., Figs. 3, 6, 9, 11, and 16). These events are almost always also observed in the C IV doublet and often in Si IV.
- The whole profile fills in, or “weakens” (λ Eri, ω Ori, and μ Cen; e.g., Figs. 4, 5, 7, and 10). This activity is largest in C IV and is occasionally visible in Si IV.
- Discrete absorptions can occur in the middle of the profile (λ Eri, ω Ori, ψ^1 Ori, and π Aqr; e.g., Figs. 4, 8, 14, and 17). Except for the 19 Mon events, these absorptions were also found in the C IV doublet.
- Short-lived, narrow emission spikes can appear in the profile (HD 67536; e.g., Fig. 12). The C IV doublet appears to

respond to these events, at least for the events observed in HD 67536.

- Extended absorption in the blue wing of $\lambda 1640$ develops at certain times in half the stars in our sample. Thus, this is the most common type of variability. The enhanced absorption is correlated with extended high velocity wind absorption in the C IV and/or Si IV doublets (ψ^1 Ori, η Cen, 2 Vul; e.g., Figs. 13, 15, and 19).

5.2. What atmospheric changes produce the $\lambda 1640$ variations?

Most of the morphologies just summarized involve similar variations in the C IV and/or Si IV doublets. Therefore, they probably reflect changes in the structures of the stars’ winds. For the spectra of λ Eri at least, we also note that some of these events correlate with the appearance of He I optical line dimples – that is, a sympathetic response in the C IV lines can also be found (Smith et al. 1996). We have stipulated that there are some He II events for which correlations with extant optical or UV data do not occur. We cannot conclude much from these particular cases.

A common event class, second in overall frequency to those displaying an extended blue wing type, is the filling of the central and red-wing profile regions, and sometimes the whole line. Attempts to interpret such events encounter the ambiguity of weakened absorption versus true emission, and thus cannot be straightforwardly attributed to changes in the wind. For example, weakened absorption might be caused by a decreased effective temperature over the visible disk, or by a decrease of the temperature gradient within the photosphere. Were either a lowering of the T_{eff} or the temperature gradient to occur for whatever reason, it would have the effect of decreasing the equivalent widths of all excited photospheric lines, as well as the wind components of the lines we have studied. This prompts the question of whether the general weakenings of the He II line also correspond to less blue wing absorption in the C IV lines. In the examples we have shown with general line weakenings, the answer seems to be “yes” in about $\frac{2}{3}$ of the cases. This includes the events shown for η Cen, 2 Vul, 19 Mon, and the Fig. 17 event for π Aqr. Thus, it appears that an argument can be made that the thermal conditions of the photosphere have a effect on the velocity and density relations of the wind.

Smith et al. (1997) have constructed non-LTE models of static atmospheres in order to examine the requirements needed to reproduce observed emissions (or absorption weakenings) in $\lambda 1640$ and the red He I lines of λ Eri. They found that emission can be produced within a moderately dense, heated slab above the atmosphere by “Lyman pumped recombination”. In this process the slab’s helium atoms feel the effects of the slab’s own Lyman continuum radiation. He I line emission will result if the slab is heated to about 50 000 K or illuminated by EUV flux having an equivalent radiation temperature. The process is efficient for a slab density of $\sim 10^{11-12} \text{ cm}^{-3}$ (which is incidentally the typical density where the line cores of the He II line are formed in B dwarf atmospheres). Moreover, the slab should be thick enough for the helium lines to be optically thick, while at same time allowing the Lyman continuum to remain thin. Such emitting structures might take the form of mild density blobs suspended above the photosphere. Equivalent conditions might be produced by a flattening of the density lapse rate in its upper regions.

What causes the filling in of the red wing of the He II line? According to VCR, a heated, isotropic wind, even with the mass loss rate expected for an early Be star, is capable of producing

visible P Cygni signatures in the He II, Si IV, and C IV lines. However, except in Fig. 12 (HD 67536) the incipient redshift emissions we have found are *not* accompanied by blueshifts of the absorption components: when the red wing is raised, the blue half of the profile is usually unchanged. This observation runs contrary to the predictions of P Cygni profiles for $\lambda 1640$ and $\lambda 4686$ from VCR models; the models predicting these features included strong, fast winds ($\dot{M} = \geq 10^{-7} M_{\odot} \text{ yr}^{-1}$) and an equivalent $\beta \ll 1$) heated to about 10000 K above T_{eff} ; see also Hamann & Schmutz (1987). Under these conditions line emission is produced efficiently because recombinations to He^{1+} are sensitive to high density and temperature. If the region coincides with the base of the wind, the acceleration of the flow reduces flux shielding in the wind, permitting more atoms to be exposed to the deep photospheric radiation flow. In Sect. 4.1 we emphasized that the red emissions of $\lambda 1640$ should not be described as true P Cygni profiles. The VCR models of $\lambda 1640$ indicate that P Cyg profiles are most easily produced if a heated chromosphere exists very close to a star.

In two of the examples we discussed, Figs. 10 and 11, the response of the C IV doublet to weak red wing emissions in $\lambda 1640$ is accompanied by increased blue wing absorption. This fits with VCR's modeling results that a heated region can be placed at a position too far from the star to influence the He II line but yet where it would be still responsible for C IV absorption in the wind. It is also important to point out that because VCR's "distant, heated wind slab" models produce red wing $\lambda 1640$ emission, one does not have to resort to ad hoc "returning blobs" to explain this emission in the observed profiles.

Before undertaking their work on the He II line, Venero et al. (2000) had produced anomalous wind models that led to absorption and emission signatures in the C IV doublet similar to those they found later for He II. Although similar models for C IV have not been explored yet by any authors, one can surmise that the responses of these lines would be similar to those just outlined. One might guess that the effects on C IV would be amplified for those models in which the wind is heated far from the star. For example, weak red wing emissions are most visible in the C IV observations – see Figs. 9, 11, and arguably 12. The mildness of this emission may be used in the future models to constrain the distance of heated regions above the star.

In addition to the wind heating requirements, the work of Venero et al. demonstrates the intuitive result that variable He II characteristics, whether in absorption or emission, increase with the mass loss rate. In cases where we have found correlated blue wing variations in both Si III and Si IV lines (e.g., Figs. 17 and 19) we estimate from tests of moving slab models using the *CIRCUS* program (Hubeny & Heap 1996) that the mass loss rate must be enhanced by a factor of at least a factor of 10. This enhancement is too large to be an effect of refocusing of wind in a magnetic dipolar field.

We have argued that the high velocity absorptions of the He II line can be best understood by a change in the mass loss rate and probably the velocity acceleration law. In addition, the most likely explanation for the faint red wing emissions is that an unknown instability, possibly magnetic, heats an accelerating region of the wind. Finally, we have suggested that conditions within the photosphere are responsible for the relatively common line weakenings across the photospheric profile.

6. Conclusions

This paper provides a mini-atlas of He II $\lambda 1640$ variability for a group of 10 Be stars selected from a much larger sample of

early-type Be, Bn, and B normal stars. We have identified several basic types of variability. Weak red emissions and line weakenings occur over timescales of a few hours or less. In terms of the variability timescales, we have noted that the pattern of strengthening blue wings occurs over long timescales. In our view this is most likely explained by changes in the wind velocity law (cause unknown). Second, line weakenings likewise occur preferentially over long timescales. Long-term weakenings occur in half of our ten $\lambda 1640$ -variable stars. Third, weakenings over the whole line or only the red wing can occur even within a few hours. We also point out that rapid variability was found preferentially in the stars η Cen and λ Eri. We believe these events speak to intrinsic properties of these stars rather than to observational sampling.

We have suggested that the properties which change the surface and wind properties of these stars are mediated by magnetic instabilities. This is among the few ways of interpreting aperiodic variations of a single star on a timescale sometimes much less than its rotation period. We note that our examples of variable $\lambda 1640$ do not include known Bp stars. Magnetic fields in these stars are thought to be dipolar and, most importantly, stable over at least several years. Strong stable fields resist the influence of hydrodynamical instabilities that might alter a wind's structure or its geometrical flow. Therefore, we conjecture that at least for some of these stars magnetic fields must be localized on the surface. Velocity perturbations due to nonradial pulsations and differential surface rotation would then offer plausible ways to trigger magnetic instabilities in these multipolar configurations.

Acknowledgements. We thank Dr. Roberto Venero for clarifications on his work on the He II $\lambda 1640$ line, Dr. Geraldine Peters for making available H α observations of ω Ori, and an anonymous referee for improving the quality of this paper.

References

- Abraham, P., Kun, P., Balazs, L., et al. 1993, A&A, 268, 230
- Abt, H., Levato, H., & Grosso, M. 2002, ApJ, 573, 359
- Auer, L. H., & Mihalas, D. 1972, ApJS, 24 193
- Baade, D., Rivinius, R., Steff, S., et al. 2001, IAUC, #7658, 2
- Balona, L. A. 1995, MNRAS, 277, 1547
- Balona, L. A., & James, D. J. 2002, MNRAS, 332, 714
- Balona, L. A., James, D. J., Motosasele, P., et al. 2002, MNRAS, 333, 952
- Barker, P. K. 1987, PASP, 95, 996
- Barker, P. K., & Marlborough, J. M. 1985, ApJ, 288, 329
- Bolton 1982, IAU Symp. 98, ed. M. Jaschek, & H.-G. Groth, (Dordrecht: Reidel), 181
- Brandt, J. C., Heap, S. R., Beaver, E., et al. 1998, AJ, 116, 941
- Brown, A., & Verschueren, W. 1997, A&A, 319, 311
- de Araujo, F. X., & de Freitas Pacheco, J. A. 1990, Ap&SS
- Christian, D. J., Craig, N., Cahill, W., et al. 1999, AJ, 117, 2466
- Cidale, L. 1993, Ph.D. Dissertation, University of La Plata
- Dachs, J., Hanuschik, R., Kaiser, D., et al. 1986, A&AS, 63, 87
- Freitas Pacheco, J. A. 1982, MNRAS, 199, 591
- Grigsby, J. A., & Morrison, N. D. 1995, ApJ, 442, 794
- Grady, C. A., Bjorkman, K. S., & Snow, T. P. 1987, ApJ, 320, 376 (GBS)
- Groote, D., & Schmitt, J. H. 2004, A&A, 418, 235
- Hanula, M. E., & Gies, D. R. 1994, IAU Symp. 162, ed. L. Balona, H. Henrichs, & J. Le Contel (Dordrecht: Kluwer), 100
- Hamann, W.-R., & Schmutz, W. 1987, A&A, 174, 173
- Hanuschik, R. 1996, A&A, 308, 170
- Hanuschik, R. W., Dachs, J., Baudzus, M., et al. 1993, A&A, 274, 356
- Hanuschik, R., Hummel, W., Sutorius, E., et al. 1996, A&AS, 116, 309
- Henrichs, H., Schnerr, R. S., & ten Kulve, E. 2005, in The Nature and Evolution of Disks around Hot Stars, ed. R. Ignace, & K. Gayley (San Francisco: ASP), ASP Conf. Ser., 337, 114
- Herrero, A. 1987, A&A, 186, 231
- Hiltner, H., Garrison, R., & Schild, R. 1969, ApJ, 157, 313
- Hummel, W., & Vrancken, M. 2000, A&A, 359, 1075
- Hubeny, I., & Heap, S. R. 1996, ApJ, 470, 1144
- Hubeny, I., Lanz, T., & Jeffery, S. 1994, Newslett. Anal. Astron. Spectra, 20, 30
- Hunter, I., Dufton, P., Ryans, R., et al. 2005, A&A, 436, 687

- Janot-Pacheco, E., Jankov, S., Leister, N. V., et al. 1999, *A&AS*, 137, 407
- Jaschek, C., & Jaschek, M. 1992, *A&AS*, 95, 535
- Irvine, N. J. 1975, *ApJ*, 196, 773
- Koubcky, P., Yang, S., Floquet, M., et al. 2005, in *Magnetic Fields on O, B, and A Stars*, ed. L. Balona, H. Henrichs, & R. Medupe (San Francisco: ASP), ASP Conf. Ser., 305, 295
- Lamers, H. J., & Waters, L. B. 1987, *A&A*, 182, 80
- Leister, N. V., Janot-Pacheco, E., Hubert, A. M., et al. 1994, *A&A*, 287, 789
- Lesh, J. R. 1968, *ApJS*, 17, 371
- Levenhagen, R. S., & Leister, N. V. 2003, *A&A*, 400, 599
- Linsky, J. L. 1998, *ApJ*, 492, 767
- Lyubimkov, L. S., Rostopchin, S., Rachkovskaya, T., et al. 2005, *MNRAS*, 358, 193
- Mennickent, R., Sterken, C., & Vogt, N. 1998, *A&A*, 330, 631
- Miroschnichenko, Bjorkman, K. S., A. S., & Krugov, V. 2002, *ApJ*, 573, 812
- Neiner, C., Hubert, A. M., Frémat, Y., et al. 2003, *A&A*, 409, 275
- Niemczura, E., & Daszynska-Daszakiewicz, J. 2005, *A&A*, 433, 659
- Pavlovski, K., Harmanec, P., Bozic, H., et al. 1997, *A&A*, 125, 75
- Percy, J., Coffin, B., Drukier, G., et al. 1988, *PASP*, 100, 1555
- Peters, G. P. 1984a, *PASP*, 96, 960
- Peters, G. P. 1984b, *ApJ*, 301, L61
- Peters, G. P. 1990, in *Angular Momentum and Mass Loss for Hot Stars*, ed. L. Willson, & R. Stalio (Dordrecht: Kluwer), ASP Conf. Ser., 316, 219
- Peters, G. P. 2005, priv. commun.
- Peters, G. P., & Gies, D. R. 2000, in *The Nature and Evolution of Disks around Hot Stars*, ed. R. Ignace, & K. Gayley (San Francisco: ASP), ASP Conf. Ser., 337, 375
- Prinja, R. K. 1989, *MNRAS*, 241, 721
- Prinja, R., Massa, D., & Fullerton, A. 2002, *A&A*, 388, 587
- Ringulet, A. E., Fontenla, J. M., & Rovira, M. 1981, *A&A*, 100, 79
- Rivinius, T., Baade, D., Stefl, S., et al. 1998a, *A&A*, 333, 125
- Rivinius, T., Baade, D., Stefl, S., et al. 1998b, *A&A*, 336, 177
- Rivinius, T., Baade, D., Stefl, S., et al. 2001, *A&A*, 369, 1058
- Rivinius, T., Baade, D., & Stefl, S. 2003, *A&A*, 411, 229
- Rivinius, T. 2005, in *The Nature and Evolution of Disks around Hot Stars*, ed. R. Ignace, & K. Gayley (San Francisco: ASP), ASP Conf. Ser., 337, 178
- Rountree, J., & Sonneborn, G. 1991, *ApJ*, 369, 515
- Shore, S. N., & Brown, D. N. 1990, *ApJ*, 365, 665
- Slettebak, A. 1982, *ApJS*, 50, 55
- Slettebak, A. 1994, *ApJ*, 194, 63
- Smith, M. A. 1989, *ApJS*, 71, 357
- Smith, M. A. 2000, in *The Be Phenomenon in Early-Type Stars*, ed. M. Smith, H. Henrichs, & J. Fabregat (San Francisco: ASP), ASP Conf. Ser., 214, 292
- Smith, M. A., & Polidan, R. P. 1993, *ApJ*, 408, 323
- Smith, M. A., Peters, G. J., & Grady, C. 1991, *ApJ*, 367, 302
- Smith, M., Grady, C., Peters, G., et al. 1993, *ApJ*, 409, L49
- Smith, M. A., Plett, K., Johns, C., et al. 1996, *ApJ*, 469, 336
- Smith, M. A., Cohen, D. H., Gu, M., et al. 1997, *ApJ*, 481, 467
- Snow, T. P. 1981, *ApJ*, 251, 139
- Sonneborn, G., Grady, C., Wu, C., et al. 1988, *ApJ*, 328, 784
- Steffl, S., Baade, D., Harmanec, P., et al. 1995, *A&A*, 294, 135
- ten Hulve, E. 2004, Masters thesis, Univ. of Amsterdam
- Venero, R. O., Cidale, L. S., & Ringulet, A. E. 2000, in *The Be Phenomenon in Early-Type Stars*, ed. M. Smith, H. Henrichs, & J. Fabregat, ASP Conf. Ser., 214, 607
- Venero, R., Cidale, L., & Ringulet, A. 1991, *ApJ*, 578, 450
- Zaal, P. A., & Waters, L. B. 1997, *A&A*, 326, 237